Chlorophyll bloom development and the subtropical front in the North Pacific

Cara Wilson,[1] Tracy A. Villareal,[2] Mark A. Brzezinski,[3,4] Jeffrey W. Krause,[3,5] and Andrey Y. Shcherbina[6]

[1] In late summer, satellite ocean color data consistently show localized chlorophyll blooms in the oligotrophic NE Pacific. Based on historical data and the results from recent cruises, these blooms are associated with elevated diatom abundance. However, the physical dynamics that stimulate the blooms remain unknown. Mechanisms suggested to be driving the blooms include mixing at the subtropical front, breaking of internal waves at the critical latitude, shoaling of the mixed layer depth, eddy interactions, and winter mixing of nutrients. To examine these hypotheses, we use data from four summer cruises (2002, 2007, 2008, and 2009) in this region that sampled near a bloom temporally and/or spatially. Conditions associated with five blooms (two blooms were sampled in 2009) are examined. Each area was sampled at a different stage in bloom development, including prebloom, initiation, full bloom, decline, and postbloom conditions. No one variable is found which can explain unequivocally the development of a chlorophyll bloom at a certain location. We describe a set of conditions that could result in the injection of nutrients into the surface water to stimulate a bloom. This "perfect storm" of conditions requires a subsurface stratification minimum layer that intersects the nutricline and that this minimum is close to the base of the mixed layer. These conditions are not predictable in the sense of an annual climatology; however, they do occur often enough to create a reasonably certain, if spatially variable, summer NE Pacific bloom.

Citation: Wilson, C., T. A. Villareal, M. A. Brzezinski, J. W. Krause, and A. Y. Shcherbina (2013), Chlorophyll bloom development and the subtropical front in the North Pacific, *J. Geophys. Res. Oceans*, *118*, 1473–1488, doi:10.1002/jgrc.20143.

1. Introduction

[2] The advent of measuring global chlorophyll from ocean color satellites led to the discovery that localized blooms consistently develop in the oligotrophic North Pacific Subtropical Gyre (NPSG) in late summer [*Wilson*, 2003; *Wilson et al.*, 2008]. These blooms can be quite extensive, covering areas of several hundred thousand square kilometers where chlorophyll concentrations are $>0.15\,\mathrm{mg\,m^{-3}}$, a value two to three times higher than background levels. Both the timing and location of these blooms are enigmatic. Phytoplankton blooms in the ocean usually occur in spring or fall, when there is temporal overlap between nutrient injection into the surface mixed layer from mixing, sufficient light levels for photosynthesis, and decreased grazing sufficient to allow net biomass accumulation [*Behrenfeld*, 2010; *Chiswell*, 2011]. However, there is no obvious mechanism of nutrient injection that fuels the summer blooms in the NE Pacific. The blooms develop in a very specific locality. The most intense and the most frequent blooms occur between 130–150°W and 28–32°N (hereinafter the 30°N blooms), but blooms also develop around Hawaii (hereinafter the Hawaii blooms) [*Dore et al.*, 2008; *Landry*, 2002; *White et al.*, 2007; *Wilson and Qiu*, 2008].

[3] While satellite data are invaluable for detecting these blooms, there are many questions that cannot be addressed by just satellite data. What are the organisms associated with these chlorophyll blooms? Are there subsurface blooms that are not detected by satellite data? Do the surface blooms have a hydrographic signature different than the nonbloom areas? Does the nutrient distribution change across the bloom boundary? To answer these questions requires in situ data. Satellite measurements of chlorophyll also underestimate the extent of the blooms in this region, as subsurface blooms have been observed near Hawaii [*Dore et al.*, 2008; *White et al.*, 2007] and along 30°N [*Villareal et al.*, 2011] that were not evident in the surface observations.

All Supporting Information may be found in the online version of this article.
[1]Environmental Research Division, Southwest Fisheries Science Center, National Marine Fisheries Service, NOAA, Pacific Grove, California, USA.
[2]Marine Science Institute and Department of Marine Science, The University of Texas at Austin, Port Aransas, Texas, USA.
[3]Marine Science Institute, University of California, Santa Barbara, California, USA.
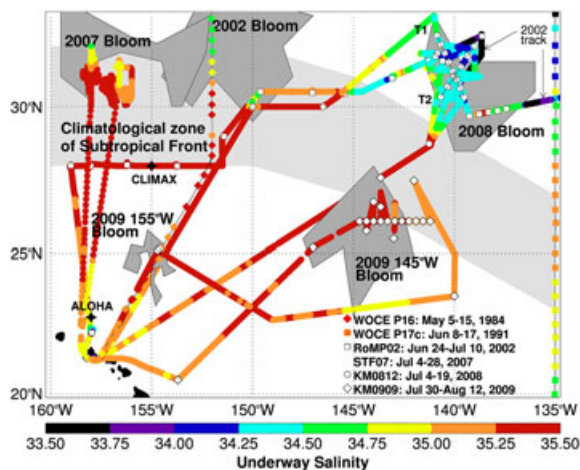[4]Department of Ecology Evolution and Marine Biology, University of California, Santa Barbara, California, USA.
[5]Dauphin Island Sea Lab, Dauphin Island, Alabama, USA.
[6]Applied Physics Laboratory, University of Washington, Seattle, Washington, USA.

Corresponding author: C. Wilson, Environmental Research Division, Southwest Fisheries Science Center, National Marine Fisheries Service, NOAA, 1352 Lighthouse Ave., Pacific Grove, CA 93950, USA. (Cara.Wilson@noaa.gov)

[4] Two long-term biological monitoring programs have been conducted in the general bloom region: the CLIMAX program collected biological data at 28°N, 155°W from 1968 to 1985 [*Venrick*, 1993], and monthly cruises to the Hawaii Ocean Time-series (HOT) station ALOHA at 22°45′N, 158°W have been conducted since 1988 (Figure 1). The CLIMAX site was located at the southwestern boundary of the region where the 30°N blooms occur, and the ALOHA station is in the region where the Hawaii blooms occur. Since the end of the CLIMAX program, there have been about 10 biological cruises along 30°N (see listings in *Dore et al.* [2008] and *Wilson et al.* [2008]). From all of these programs, we know that summer blooms of diatom-diazotroph assemblages (DDAs), as well as other diazotrophs, occur in both regions [*Brzezinski et al.*, 2011; *Dore et al.*, 2008; *Heinbokel*, 1986; *Karl et al.*, 2012; *Venrick*, 1974]. Blooms of the diazotroph *Trichodesmium* have been observed near Hawaii [*Guidi et al.*, 2012; *Karl et al.*, 1992; *Sohm et al.*, 2011], but not near 30°N [*Venrick*, 1997; *Villareal et al.*, 2011; *Wilson et al.*, 2008]. The abundance of vertically migrating mats of *Rhizosolenia* is higher along 30°N [*Wilson et al.*, 2008]. Subsurface (100–150 m depth) biomass levels at CLIMAX are higher than those off Hawaii [*Venrick*, 1997]. Diazotrophs can thrive in nitrate-deplete waters by their ability to fix nitrogen, but there must be sufficient amounts of phosphate, iron, and—in the case of diatoms—silicon. In the bloom region, phosphate appears to be the limiting nutrient for diazotrophs [*Dore et al.*, 2008]. Diazotrophy is energetically costly [*Karl et al.*, 2002], and the seasonal timing of the blooms is probably driven by the increased light energy in the summer.

[5] The physical dynamics which stimulate the blooms remain unknown, although multiple hypotheses have been put forth to explain the blooms' development. Dynamics associated with the convergent zone [*Wilson et al.*, 2008], the subtropical front (STF) [*Wilson*, 2003; *Wilson and Qiu*, 2008], the breaking of internal waves at the critical latitude [*Wilson*, 2011], eddy interactions [*Fong et al.*, 2008; *Guidi et al.*, 2012], and winter mixing of phosphate into the mixed layer [*Dore et al.*, 2008] have all been suggested as mechanisms driving the blooms. Blooms occur when the mixed layer is shallow (<70 m), but these conditions often occur without the development of a bloom [*Dore et al.*, 2008; *Villareal et al.*, 2012; *White et al.*, 2007]. The Hawaii blooms develop when the sea surface temperature (SST) is between 25°C and 27°C [*White et al.*, 2007], while the 30°N blooms occur within a much wider SST range, from 20°C to 26°C [*Villareal et al.*, 2012].

[6] Doming of isopycnals in eddies has been observed to coincide with enhanced phytoplankton biomass, and much work has focused on these interactions in the lee of the Hawaiian Islands [*Benitez-Nelson and McGillicuddy*, 2008]. While this dynamic has been observed at ALOHA [*Letelier et al.*, 2000], most of the NPSG blooms north of Hawaii do not follow this scenario. The blooms cover areas of several hundred thousand square kilometers, which are much larger than the spatial scale of eddies. The blooms are most often wrapped around eddies [*Guidi et al.*, 2012; *Wilson and Qiu*, 2008], and it appears that the chlorophyll field is stretched out by the flow field [*Calil et al.*, 2011; *Calil and Richards*, 2010]. While the eddy kinetic energy just north of Hawaii is significantly stronger than that at 30°N [*Calil and Richards*, 2010], the Hawaii blooms are generally weaker and more diffuse than those at 30°N [*Dore et al.*, 2008; *Krause et al.*, 2013; *Wilson and Qiu*, 2008]. Blooms of DDAs have been observed at HOT associated with anticyclonic eddies [*Church et al.*, 2009; *Fong et al.*, 2008].

[7] Since the 30°N blooms consistently develop at the same latitude where the STF occurs [*Roden*, 1975, 1980] and oceanic fronts are often associated with enhanced biological activity [*Franks*, 1992; *Liu and Woods*, 2004; *Olson*, 2002; *Stumpf et al.*, 2008; *Yoder et al.*, 1994], a mechanistic link between the two features is suggested. However, the presence of the front alone is not sufficient to explain the appearance of the blooms, as the STF is a relatively uniform feature across the Pacific Basin, and the blooms develop preferentially in the eastern half of the Pacific [*Wilson et al.*, 2008]. Satellite-observed open-ocean chlorophyll blooms rarely develop west of the Hawaiian Ridge (one did in 2010 [*Calil et al.*, 2011] and 2012), although diatom blooms have been observed in the central Pacific that did not have a satellite chlorophyll signal [*Villareal et al.*, 2011]. The basin-wide distribution of the satellite chlorophyll blooms is probably driven in part by the shallower nutricline in the eastern half of the Pacific [*Dore et al.*, 2008; *Wilson et al.*, 2008]. While both features, the STF and the blooms, generally occur near 30°N, the exact position of both can vary by several degrees of latitude each year [*Laurs and Lynn*, 1977; *Saur*, 1980; *Seki et al.*, 2002; *Wilson and Qiu*, 2008].

[8] The occurrence of the blooms in the eastern part of the NPSG has been attributed to the breaking of internal waves (IWs), generated at Hawaii, when they arrive at the critical latitude of 30°N [*Wilson*, 2011]. Dynamics of IWs are

Figure 1. Schematic representation of the locations of the satellite chlorophyll blooms in 2002, 2007, 2008, and 2009, overlain with cruise sampling locations and underway shipboard salinity data. The 2007 cruise used a towed instrument and did not have distinct stations. The cruises in 2002 and 2007 sampled independently of the satellite chlorophyll data, whereas the 2008 and 2009 cruises were specifically targeting blooms. The climatological region of the STF (modified from *Roden* [1975]) is shown in light gray. Sampling dates (not cruise dates) are listed on the figure. Surface salinity data from two WOCE sections through this region are shown as color-coded circles along the transect lines.

strongly dependent on the background stratification, and internal wave breaking and turbulent mixing will be facilitated in regions with low stratification. A subsurface stratification minimum (SSM) occurs in the bloom region in the summertime, at a depth that would create mixing between the surface water and the nutricline [*Wilson*, 2011]. The SSM only develops in the region where the blooms develop (130–150°W), further explaining the blooms' distribution in the eastern part of the Pacific.

[9] Here, data from four cruises, one each in 2002, 2007, 2008, and 2009, are used to examine the hypotheses that the 30°N blooms develop (1) at the STF and (2) where there is a SSM. The four cruises all had different scientific objectives, none of which were aimed at specifically addressing these questions. However, all cruises collected hydrographic data in the vicinity of a chlorophyll bloom, thereby enabling these questions to be addressed. The 2008 and 2009 cruises were the first cruises that specifically targeted sampling of the summer chlorophyll blooms at 30°N, though the 2002 cruise serendipitously sampled one. Each area sampled was at a different stage in bloom evolution: either in a prebloom, initiation, full bloom, decline, or postbloom condition. The focus here is on blooms near 30°N; however, one of the blooms sampled occurred at 25°N, about halfway between the ALOHA station and 30°N. In section 2, the cruises and the supplementary data sources used are described. In section 3, the results from the cruises are presented separately, followed by a discussion in section 4 and conclusions in section 5.

2. Data

2.1. Cruise Data

[10] The sampling schemes of the four cruises are shown in Figure 1, as well as schematic locations of the chlorophyll blooms in each of those years and the climatological region of the STF. In summer, the STF is best identified by surface salinity data as a south-north decrease in salinity near 30°N [*Roden*, 1974]. Since most of the cruises had a relatively small study area, the underway salinity data for the entire cruise tracks are shown to better identify the position of the STF. For additional regional perspective, surface salinities from the two summer World Ocean Circulation Experiment (WOCE) sections through the area are also shown in Figure 1. Ship sensors were calibrated as per UNOLS requirements by the ship's technical support teams.

2.1.1. R/V *Melville* (RoMP02) Cruise

[11] The RoMP02 cruise took place on the R/V *Melville* between 20 June and 16 July 2002 and sampled the eastern North Pacific between Hawaii and San Diego along roughly 30°N (Figure 1 and Table 1). This cruise was part of the *Rhizosolenia* Mats in the Pacific (RoMP) project and was aimed at quantifying nitrogen importation and excretion in the euphotic zone by vertically migrating *Rhizosolenia* mats [*Pilskaln et al.*, 2005; *Singler and Villareal*, 2005; *Villareal et al.*, 2011].

2.1.2. R/V *Wecoma* (STF07) Cruise

[12] The STF07 cruise took place on the R/V *Wecoma* between 5 and 29 July 2007 near 31°N, 158°W (Figure 1 and Table 1) and was aimed at investigating the distribution and structure of thermohaline intrusions within the STF [*Shcherbina et al.*, 2009, 2010]. The hydrographic survey

Table 1. Summary of Cruises Whose Data Are Used Here

Ship (Cruise)	Dates	References
R/V *Thomas Washington* (WOCE P16)	May 1984	[*Talley et al.*, 1991]
R/V *Thomas Washington* (WOCE P17c)	Jun–Aug 1991	[*Tsuchiya and Talley*, 1996]
R/V *Melville* (RoMP02)	20 Jun to 16 Jul 2002	[*Pilskaln et al.*, 2005; *Singler and Villareal*, 2005; *Villareal et al.*, 2011; *Wilson et al.*, 2008]
R/V *Wecoma* (STF07)	4–28 Jul 2007	[*Shcherbina et al.*, 2009, 2010]
R/V *Kilo Moana* (KM08)	1–22 Jul 2008	[*Duhamel et al.*, 2010; *Krause et al.*, 2012, 2013;
R/V *Kilo Moana* (KM09)	29 Jul to 14 Aug 2009	*Li et al.*, 2011; *Villareal et al.*, 2012; *Watkins-Brandt et al.*, 2011]

was conducted with a depth-cycling towed instrument platform. The overall survey was guided by near-real-time satellite SST data. While seasonal warming often precludes the front from being detected by SST data, there was sufficient correspondence of the surface temperature features with the structure of the thermocline fronts to make SST imagery useful in focusing the observations [*Shcherbina et al.*, 2009]. No nutrient or biological data were collected on this cruise.

2.1.3. R/V *Kilo Moana* (KM08) Cruise

[13] Two cruises on the R/V *Kilo Moana* in 2008 and 2009, KM08 and KM09, were made to investigate silicon cycling in the Pacific [*Krause et al.*, 2012; *Villareal et al.*, 2012]. The objective of these cruises was to sample satellite ocean color features for phytoplankton biomass and species composition, and daily satellite ocean color imagery was used to determine the station sampling. Nutrient data have been reported elsewhere [*Krause et al.*, 2012, 2013; *Villareal et al.*, 2012], and details of the methodologies and calibration can be found there. The KM08 cruise took place on 1–22 July 2008 near 31°N, 140°W (Figure 1 and Table 1). A chlorophyll bloom was developing as the ship left port on 1 July 2008 and was sampled during the cruise. Two intersecting transects were made through the center of the bloom. During the cruise, salinity mapping was performed at night using the ship's underway system to obtain a broader geographical view of the salinity field (Figure 1).

2.1.4. R/V *Kilo Moana* (KM09) Cruise

[14] The KM09 cruise took place on 29 July to 14 August 2009 near 26°N, 141–145°W (Figure 1 and Table 1). During this cruise, one transect was conducted along 26°N near 145°W, which was the region of a large chlorophyll bloom that had collapsed a week prior to occupation. A small chlorophyll bloom developed during the cruise further south near Hawaii at 155°W, and two stations were occupied in this active bloom during its peak.

2.2. WOCE Data

[15] Data from two summer WOCE transects in the NE Pacific were used to show snapshots of the STF within the bloom region. The P16 cruise was conducted on the R/V *Thomas Washington* on 5 May to 5 June 1984 along 152°W, and the P17c cruise was conducted on the R/V

Thomas Washington on 31 May to 11 July 1991 along 135°W (Figure 1 and Table 1).

2.3. Argo Data

[16] Argo float data were used to provide additional observations of stratification and hydrographic variability within the region. Data were examined from Argo floats 5900674, 5900887, and 5901757, which were near chlorophyll blooms in the summers of 2008 and 2009. Float 5900887 drifted from east to west south of the 2008 bloom, float 5900674 drifted across the northern part of the KM08 transects, and float 5901757 drifted from east to west north of the 2009 bloom at 155°W.

2.4. Satellite Data

[17] Ocean color data from both the Moderate Resolution Imaging Spectroradiometer (MODIS) sensor on NASA's Aqua satellite and from the Sea-viewing Wide Field-of-view Sensor (SeaWiFS) on GeoEye's OrbView-2 satellite were used to map the satellite chlorophyll blooms. For the 2008 and 2009 cruises, which were guided by daily ocean color imagery, the west coast regional node of NOAA's CoastWatch program processed the MODIS data and sent them to the ship every day. The 2002 cruise occurred the same week that the MODIS/Aqua satellite started collecting data. Therefore, SeaWiFS data were used to examine the development of the 2002 bloom. A chlorophyll value of 0.15 mg/m^3 was used as a threshold to indicate bloom conditions, based on previous work in this region [*Wilson*, 2003; *Wilson et al.*, 2008].

[18] SST data from the Advanced Microwave Scanning Radiometer-Earth Observing System (AMSR-E) instrument on NASA's Aqua satellite were used to provide additional information about conditions during the 2008 bloom. The AMSR-E instrument operates in the microwave frequency and thus is able to measure through clouds to produce daily images that are relatively complete, though of lower spatial resolution than infrared satellite SST measurements.

[19] Sea surface height anomaly (SSHA) data from AVISO (Archiving, Validation and Interpretation of Satellite Oceanographic data) were used to map the eddy field around the chlorophyll blooms. All satellite data were obtained from the ERDDAP (Environmental Research Division's Data Access Program) server at NOAA's Environmental Research Division.

3. Results

[20] Here we will show the data from the four cruises, examining whether the 30°N blooms develop (1) at the STF and (2) where there is a SSM. However, since most of the cruises did not have sampling strategies designed to map out the STF, WOCE data are presented first to show transects across it at 152°W and 135°W (Figure 2).

3.1. STF Description

[21] The STF is one of a number of fronts in the transition zone between the cold, low-salinity polar water of the Subpolar Gyre and the warm, high-salinity subtropical water of the North Pacific Subtropical Gyre. In addition to the STF
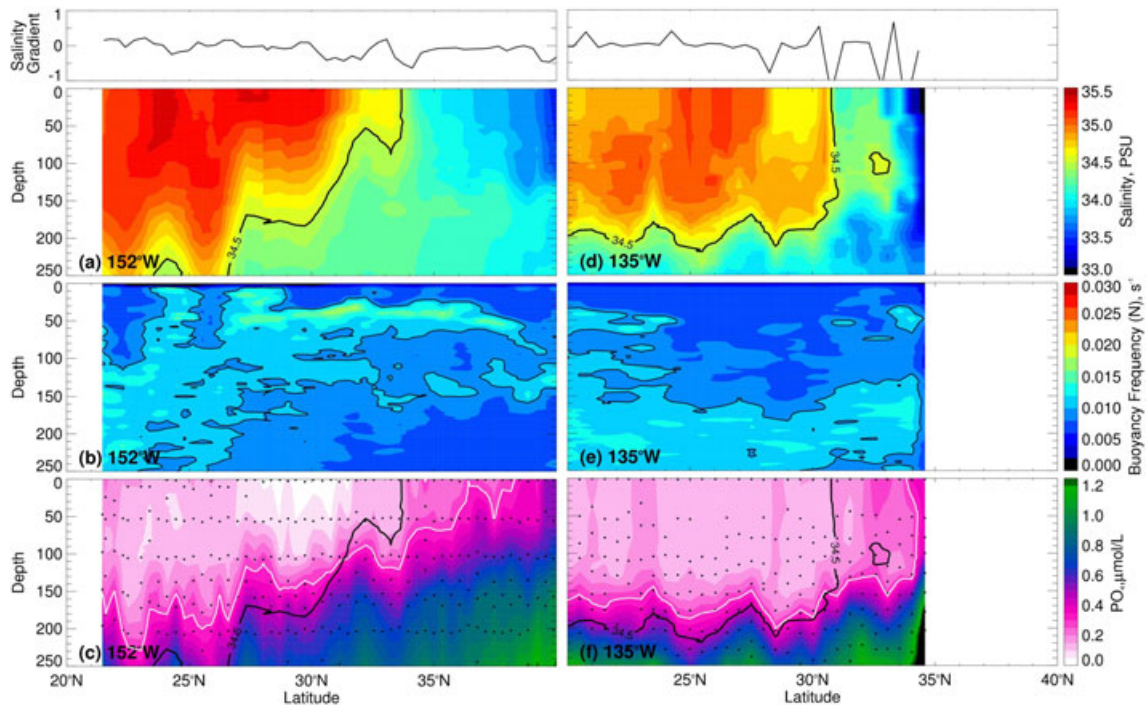
Figure 2. Data from two WOCE sections through the bloom region showing the (a) salinity, (b) buoyancy frequency N (s^{-1}), and (c) phosphate (μM) distribution in the upper 250 m along 152°W and the (d) salinity, (e) buoyancy frequency N (s^{-1}), and (f) phosphate (μM) distribution in the upper 250 m along 135°W. The 34.5 isohaline, which best represents the position of the front, is overlain on the plots. The white lines in Figures 2c and 2f are the 0.3 μM isoclines. The salinity gradient (1/degree latitude) is shown above Figure 2a and Figure 2d.

at 30°N, there is a South Subtropical Front at approximately 28°N, the North Subtropical Front (NSTF) at 34°N, and the Subpolar Front at 40°N [*Lynn*, 1986; *Roden*, 1980; *Seki et al.*, 2002]. The latitudes of the fronts are approximate as they shift seasonally, interannually, and longitudinally. Going eastward across the Pacific, the fronts start to curve southward at about 140°W [*Roden*, 1971, 1974, 1975]. The blooms generally develop at or slightly north of 30°N, placing them in the region of the STF and the NSTF (Figure 1). Unlike the STF, the NSTF (also called the 34°N front) has not been discussed much in the literature [*Lynn*, 1986; *Roden*, 1980; *Seki et al.*, 2002], and it is also possible that it does not exist every year. There is considerable interannual and seasonal variability in the strength and position of the frontal region; as many as three separate salinity fronts have been observed, and sometimes none [*Saur*, 1980]. Consequently, a "frontal zone" rather than a specific front is the more accurate description [*Samelson and Paulson*, 1988]. While the fronts generally have a characteristic salinity and temperature, there is considerable temporal and spatial variation in those values. Additionally, salinity decreases to the east along the front [*Niiler and Reynolds*, 1984]; hence, a specific salinity will not delineate it in all places, at all times. We use either the 34.5 or 35.0 isohalines to delineate the STF as appropriate.

[22] The STF was spread out in the WOCE section along 152°W, with a surface expression between 0 and 50 m depth at 34°N and a subsurface salinity front between 50 and 200 m depth spanning 30–34°N (Figure 2a). The 34.5 isohaline best marked the position of the front. Along 135°W, the STF was more tightly confined, occurred between 30°N and 31°N, and was manifest throughout the upper 200 m (Figure 2d). The fronts were also indicated by spikes in the surface salinity gradient (Figures 2a and 2d).

[23] The stratification was different between the two sections. Along 152°W the maximum stratification (highest buoyancy frequency) occurred primarily at ~50 m depth, while along 135°W it was at ~200 m depth. Along 152°W, there was a slight increase in stratification near 150 m depth on the northern side of the front between 33°N and 39°N, creating a local minima, a SSM, at ~100 m depth (Figure 2). Along 135°W, there were two areas with a SSM, one northward of the STF and one between 20°N and 24°N. These sections were taken in different years (1984 and 1991), and hence, the variability could be temporal or spatial. However, the key point is that in both sections there was a SSM at the front.

[24] Along the 152°W transect, there was a shoaling of the phosphacline (represented by the 0.3 μmol/kg isocline) across the STF (Figure 2c). At the southern end of the transect, north of Hawaii, it was at ~250 m depth and it outcropped at the surface north of the front at 35°N. The shoaling was gradual along the transect, with no indication of a front in the nutrient distribution between 31°N and 34°N as there was in the salinity section. In contrast, in the 135°W section, there was no change in the nutricline depth across the STF, but a sharp nutrient front several degrees north of the front (Figure 2f). Both sections showed a slight increase in surface phosphate on the northern side of the STF. This pattern of a gradual northward shoaling of the nutricline across the subtropical gyre and outcropping between 35°N and 40°N is consistent with previous observations [*Hayward et al.*, 1983; *Pak et al.*,

1988]. The nitrate data had similar patterns across both sections (Figure S1 in the auxiliary material), except that there was no increase of surface nitrate north of the front. However, *Seki et al.* [2002] did observe a surface increase of nitrate at the STF in the spring.

3.2. RoMP 2002 Cruise

[25] The RoMP02 cruise transected the eastern North Pacific between Hawaii and San Diego along roughly 30°N (Figure 1 and Table 1). Satellite data were not used to guide station placement during the RoMP02 cruise, but the cruise track fortuitously sampled the southern boundary of a chlorophyll bloom as observed from satellites (Figure 3). The cruise stations occurred at the beginning of the increase in chlorophyll level, i.e., at the bloom initiation stage (Figure 3a). The bloom peaked approximately 3 weeks after the sampling. The SSHA associated with the bloom ranged from −2 to +12 cm, and the bloom was not focused within eddy centers.

[26] The bloom occurred in the eastern part of the general study area, i.e., in the area where the STF curves southward, and hence, the front can be observed in a longitudinal transect. The RoMP02 cruise traversed a sharp surface salinity front near 139°W (Figure 4a). At this location, the cruise track went north and the transect changed direction from being west-to-east to being south-to-north (see Figure 1), during which the front was crossed again, resulting in the complicated structure seen in the salinity section (Figure 4a). The front extended vertically throughout the surface 200 m of water. As with the WOCE data, the 34.5 isohaline best marks the position of the front. The front was also clearly visible from the ship as a large slick perpendicular to the ship's course and extending across the entire visible horizon
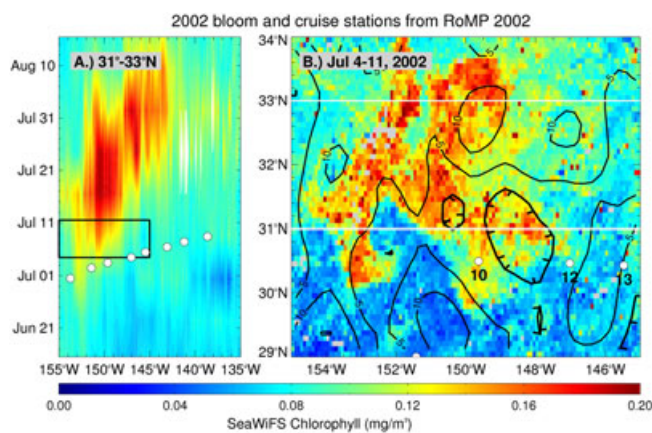
Figure 3. Hovmöller diagram of (a) SeaWiFS chlorophyll showing the development of the 2002 bloom and (b) an 8 day composite (4–11 July) showing the maximum extent of the chlorophyll bloom, overlain with station locations (circles) and SSHA contours. The zero contour is thicker and has hash marks indicating the direction of negative values. The contour interval is 5 cm. The black lines in Figure 3a depict the temporal and longitudinal extent of the data shown in Figure 3b, and the white lines in Figure 3b depict the latitude range of the data shown in Figure 3a. Gray areas have missing data due to cloud coverage.
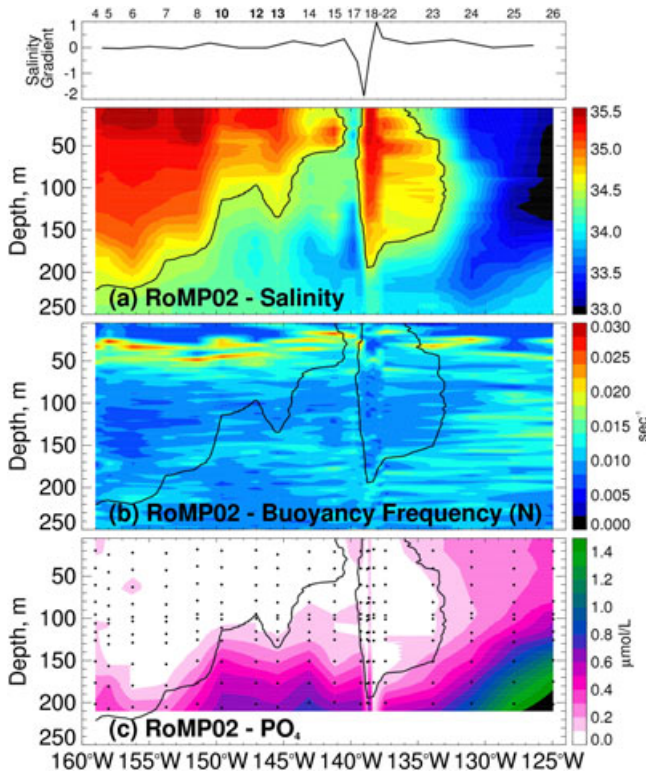
Figure 4. Sections of (a) salinity, (b) the buoyancy frequency N (sec^{-1}), and (c) phosphate (μM) for the RoMP02 cruise, along roughly 30°N (see Figure 1). The station sampling is shown by the station numbers along the top of Figure 4a and by positions of the bottle samples marked by the black dots in Figure 4c. The three stations in bold text were closest to the satellite blooms as seen in Figure 2. The black line is the 34.5 isohaline. The surface salinity gradient (1/degree longitude) is shown above Figure 4a.

(Figure 5). The frontal zone extended from 140°W to about 150°W, although between 145°W and 150°W, the front was manifest primarily in the subsurface, as seen by the almost vertical isohalines between 50 and 150 m depth at 150°W (Figure 4a). There was a SSM along most of the section, extending between 135°W and 160°W at 100–150 m depth (Figure 4b). The phosphacline (Figure 4c) ranged between 150 and 200 m depth across the section between 135°W and 160°W. As the transect left the subtropical gyre and entered into the California Current near 135°W, the nutricline shoaled sharply.

[27] There were no elevated biological signals at the surface salinity front at 140°W, in either the satellite data or in the in situ data [*Villareal et al.*, 2011]. A significant bloom of diatoms containing *Richelia*, a nitrogen-fixing endosymbiont, occurred between 146°W and 150°W (stations 10–13, see Figures 3b and 4), just on the saltier side of the front [*Villareal et al.*, 2011; *Wilson et al.*, 2008]. This diatom bloom occurred in the region where the phosphacline was relatively shallow, ~150 m depth although the bloom itself was centered in the upper 75 m. These stations were within the southern extent of the satellite chlorophyll bloom and were occupied about 2 weeks before the maximum chlorophyll signal observed in the satellite data (Figure 3).
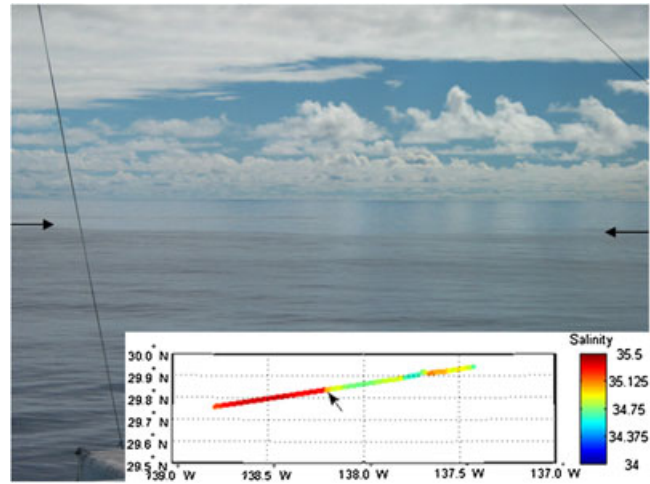
Figure 5. Photograph (contrast enhanced) of the subtropical front taken on 10 July 2002 at 29°50.564′N, 138°08.867′W on cruise RoMP02 (between stations 20 and 21). Arrows in the photograph indicate the location of the front, which was visible from horizon to horizon as a sharp change in surface texture. Underway data highlight the abrupt salinity change that occurred at the frontal boundary (arrow) depicted in the photograph.

3.3. STF07 Cruise

[28] Data from the STF07 cruise provide a look at conditions prebloom, as a chlorophyll bloom developed at the location of the ship survey about a month afterward (Figure 6a). The SSHA associated with the initial bloom ranged from 0 to 8 cm, and the bloom was not focused within eddy centers.

[29] Two distinct fronts were sampled during STF07 along the 158°W transect, one at 31°N and another at 31.5°N (Figure 7a). As observed in 2002, the fronts had different vertical structures. The southern salinity front was nearly vertical down to below 120 m depth, whereas at the northern front the salinity gradients weakened considerably below 40 m depth. The front, marked by the 35 isohaline, was slightly saltier than that in the WOCE and RoMP sections where it was marked by the 34.5 isohaline. However, this is consistent with the front being saltier in the western Pacific [*Niiler and Reynolds*, 1984], as the STF07 cruise was the furthest west of the four cruises (Figure 1).

[30] There is no indication of a SSM along the STF section (Figure 7b). The data only go down to 150 m depth, the typical depth of the SSM in this area [*Wilson*, 2011], making it possible that the sampling was not deep enough to fully resolve a SSM. However, another shorter section taken during the STF07 cruise sampled to 250 m depth, and there was no SSM observed (Figure S2).

[31] There was no chlorophyll bloom in the region at the time of the STF07 cruise in July 2007. In early August, approximately a month after the cruise, a bloom started to develop in the location of the study area, just west of the sample tracks (Figure 6b). This bloom went on to develop into one of the largest satellite-observed chlorophyll blooms in this region [*Wilson and Qiu*, 2008].

3.4. KM08 Cruise
3.4.1. KM08 Transects

[32] A chlorophyll bloom was developing as the ship left port on 1 July 2008, but it had passed its peak by the time
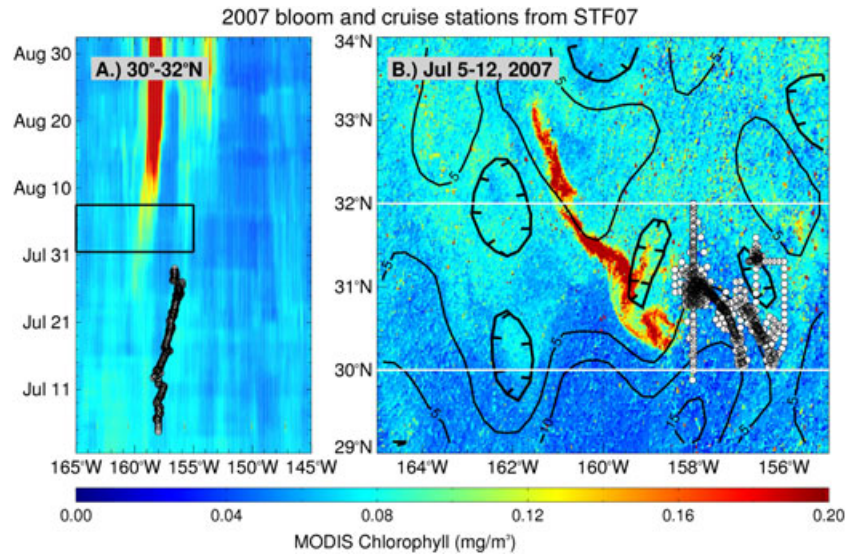
Figure 6. Hovmöller diagram of (a) MODIS chlorophyll showing the development of the 2007 bloom and (b) an 8 day composite (28 July to 4 August) showing initiation of the chlorophyll bloom, overlain with tracks of the towed instrument and SSHA contours. The zero contour is thicker and has hash marks indicating the direction of negative values. The contour interval is 5 cm. The black lines in Figure 6a depict the temporal and longitudinal extent of the data shown in Figure 6b, and the white lines in Figure 6b depict the latitude range of the data shown in Figure 6a.
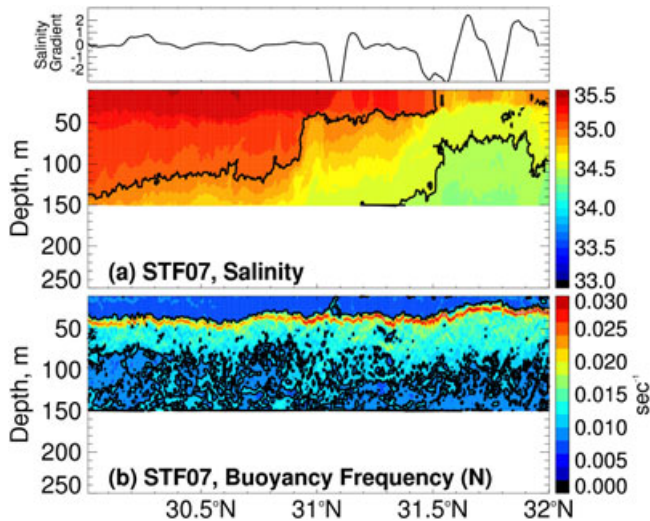
Figure 7. Sections of (a) salinity and (b) the buoyancy frequency N (s^{-1}), along 158°W taken on 5 July 2007 on the STF07 cruise. Black lines show the 34.5 and 35.0 isohalines. While the data only extends to 150 m, the plots are scaled to 250 m for consistency with data from the other cruises. The surface salinity gradient (1/degree latitude) is shown above Figure 7a.

the ship arrived at the bloom location (Figure 8). Although the bloom was in decline, bloom-level diatom biomass was observed at several stations [*Krause et al.*, 2012, 2013; *Villareal et al.*, 2012]. Unlike the other blooms, the 2008 bloom was focused within the center of an anticyclonic eddy. The SSHA associated with the bloom ranged from +2 to +14 cm.

[33] The KM08 cruise focused on sampling within the bloom region, and the survey pattern did not provide complete resolution of the structure of the front. The clearest indication of the location of the STF during the KM08 cruise came from the underway salinity data (Figure 1). The target sampling area, determined by near-real-time satellite chlorophyll data, coincided with the STF, as seen by surface salinities < 34.75 (Figure 1). Two intersecting transects were made through the center of the bloom feature (Figure 8). Because both of these transects were within the frontal zone, the salinity sections (Figures 9a and 9d) include a southern station outside the bloom and frontal region for context (see Figure 8b).

[34] The front was evident just north of 31°N and was best marked by the 34.5 isohaline (Figures 9a and 9d). There was variability in the vertical extent of the low-salinity layer associated with the front; in some stations it extended to 200 m depth (stations 5, 6, 16–18), while in others it was manifest only in the top 50 m (stations 9–12, 19–21). In transect 1 (Figure 9a), the front appeared as a meander, or as a "plug" of low-salinity water, between 31°N and 32°N. This feature will be discussed in further detail in the next section.

[35] Within the frontal zone, there was a SSM between 50 and 150 m depth. (Figures 9b and 9e). While it existed across the entire region, it was the strongest and shallowest at the frontal zone between 31°N and 32°N.

[36] Surface nutrient levels were low, mostly at the level of detection across most of the region (Figures 9c and 9d). The phosphacline was only sampled in the northernmost stations of both transects, coincident with the front, where P levels increased below 140 m. It is interesting to note that the stations within the salinity plug had higher levels of phosphate up to 50 m depth. There was no corresponding feature evident in the nitrate + nitrite data (Figure S3).
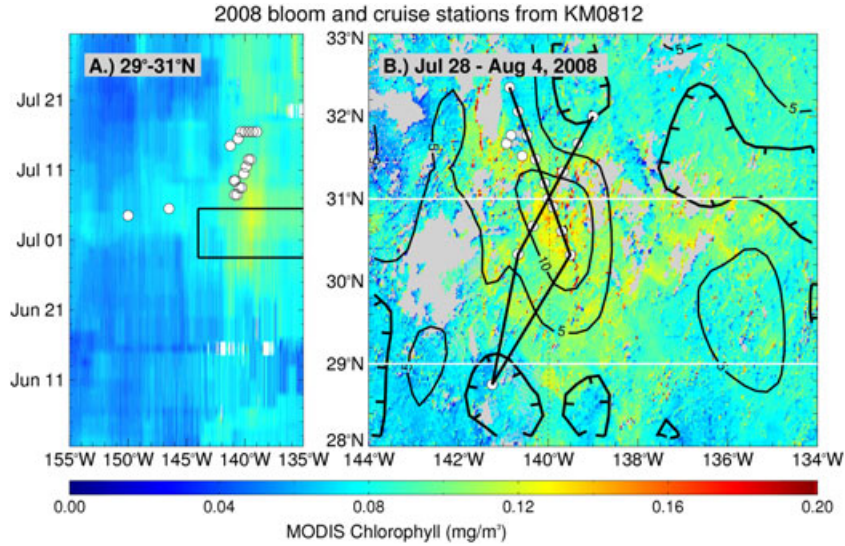
Figure 8. Hovmöller diagram of (a) MODIS chlorophyll showing the development of the 2008 bloom and (b) an 8 day composite (25 June to 2 July) showing the maximum extent of the chlorophyll bloom (about a week prior to sampling), overlain with station locations (circles) and SSHA contours. The zero contour is thicker and has hash marks indicating the direction of negative values. The contour interval is 5 cm. The white lines in Figure 8a depict the temporal and longitudinal extent of the data shown inFigure 8b, and the white lines in Figure 8b depict the latitude range of the data shown in Figure 8a. Gray areas have missing data due to cloud coverage.
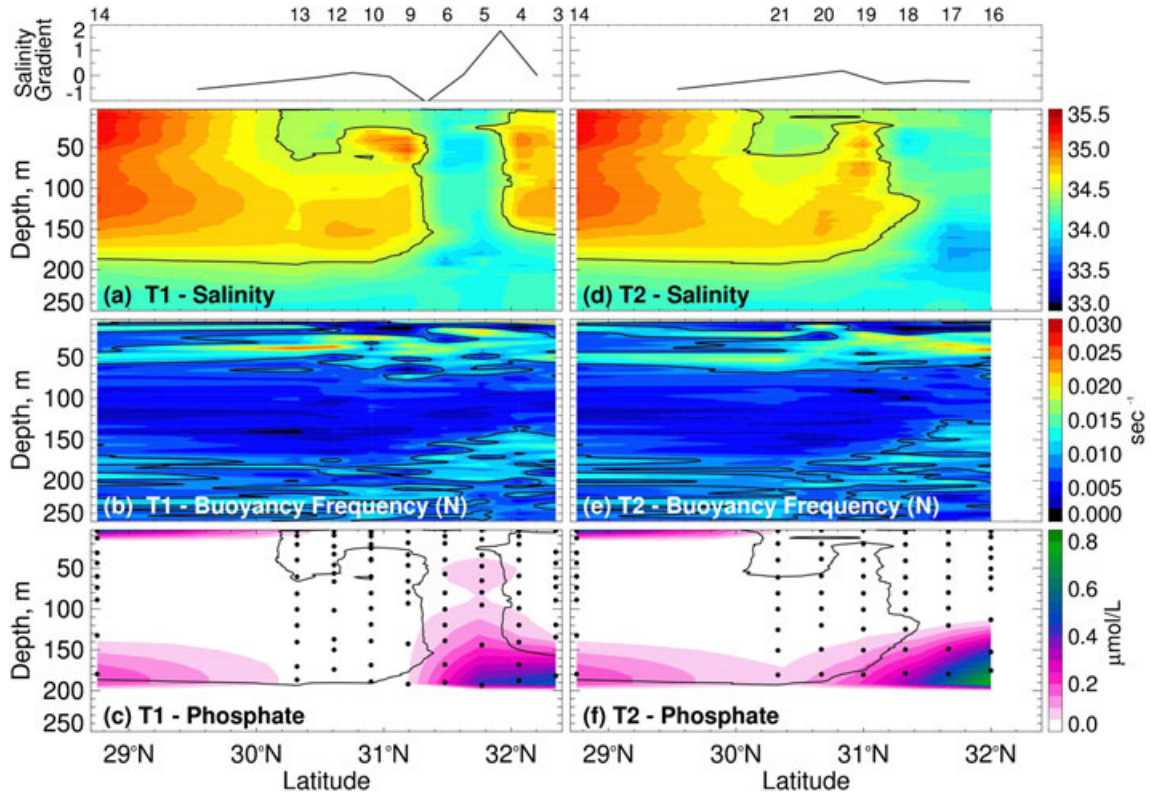
Figure 9. Sections of (a) salinity, (b) the buoyancy frequency N (s^{-1}), and (c) phosphate (μM) from KM08 transect 1 and sections of (d) salinity (PSU), (e) the buoyancy frequency N (s^{-1}), and (f) phosphate (μM) from KM08 transect 2. The station sampling is shown by the station numbers along the top of Figures 9a and 9d and by positions of the bottle samples marked by the black dots in Figures 9c and 9f. The black line is the 34.5 isohaline. The surface salinity gradient (PSU/degree latitude) is shown above Figure 9a and 9d.
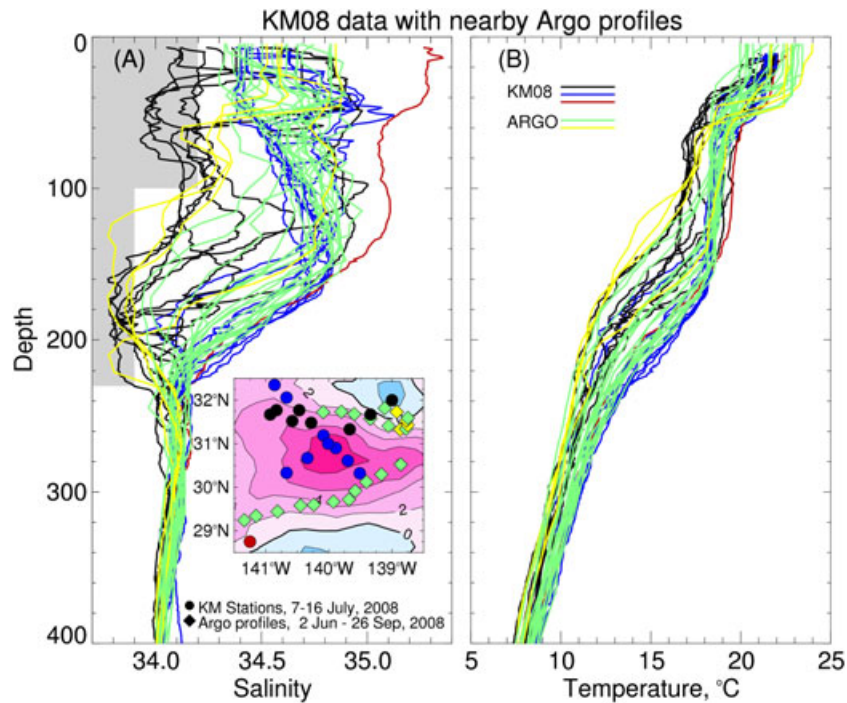
3.4.2. Salinity Profiles

[37] The salinity profiles from KM08 can be grouped into three types (Figure 10a). Salty surface water ($S > 35$) indicative of the subtropical gyre occurred south of the study area (colored red in Figure 10); at the bloom site, there were both low-salinity ($S < 34.3$) surface water (colored black) and a transitional type (colored blue) between these two end points. As seen in the salinity contours (Figure 9), the frontal structure was complicated, and the transects appeared to sample different parts of a low-salinity meander or an eddy in the frontal zone. This meander is better visualized by the map inset in Figure 10a showing the locations of the fresher water (black) relative to the intermediate water (blue).

[38] Two Argo buoys drifted through the study region during the summer of 2008, and profiles from these buoys and their locations are also shown in Figure 10. The Argo buoy that drifted south of the bloom site between 29°N and 31.5°N sampled only intermediate salinities (green profiles). The buoy that drifted along the northern part of both KM08 transects sampled both relatively fresh ($S < 34.3$, yellow) and intermediate ($S > 34.3$, green) salinities. The fresher salinities all occurred near 139°W and 31.5°N. The buoy changed course in this area, and seven profiles were taken closely clumped together between 15 July and 15 September 2008. Despite their spatial proximity, these profiles had considerable variability in salinity, with no clear spatial or temporal pattern to the occurrence of fresher versus intermediate profiles.

[39] There was also a small anticyclonic eddy in the study area. The eddy, clearly visible in satellite SSHA data (Figures 8 and 10a inset), started to develop at this location in April and by the end of August was engulfed by higher SSH which developed around it (Figure S4). However, it appears that the local hydrography is driven by frontal dynamics more than by eddy dynamics. If the eddy was driving the hydrography, the salinity distribution across the eddy should be more symmetrical. The low salinities along the northern edge of the eddy were most likely caused by a frontal intrusion as can be seen in the AMSR-E SST data (Figure 11). In the summer, SST is generally considered a poor indicator of the STF, and the temperature data from KM08 and the Argo floats show very little variation (Figure 10b). However, *Shcherbina et al.* [2009] were successful in using SST as a proxy for the STF. When transect 1, the section with the fresh salinity plug, was being conducted (7–12 July), there was a tongue of colder water intruding from the east across the northern part of the transects, as depicted by the 21.5° isotherm (Figure 11a), consistent with data from the salinity transects. The colder water is not associated with the eddy for two reasons. It is not a consistent feature throughout the summer, whereas the eddy was visible in SSH data for several months (Figure S3), and anticyclonic eddies have warm cores, not cold cores. This feature was not present a week later when transect 2 was conducted (Figure 11b), but similar intrusions of cold water across the front were present in other areas. There was also a tongue of warm water extending northeast just north of the bloom site. This high degree of spatial and temporal variability of the front's location is consistent with the variability observed in the salinity data from the Argo

Figure 10. Profiles of (a) salinity and (b) temperature from the KM08 cruise and from two nearby Argo floats. The station with a surface salinity above 35 is red, the stations with lower salinities are black (KM08) and yellow (Argo), and the intermediate stations are blue (KM08) and green (Argo). Lower salinity profiles were defined as $S < 33.9$ below 100 m depth or $S < 34.2$ in the surface layer (shown by the gray area). The inset shows the locations of the KM08 stations (circles) and the Argo floats (diamonds), overlain on contours of SSHA from 7 to 27 July 2008. The contour interval is 2 cm.
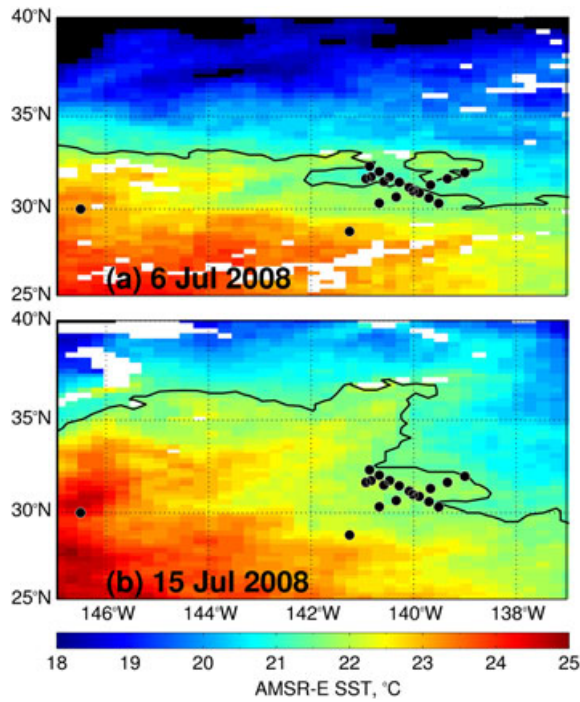
Figure 11. Maps of daily images of SST data from AMSR-E on (a) 6 July 2008, the time period of transect 1 from KM08, and (b) 15 July 2008, the time period of transect 2 from KM08. The station positions from KM08 are shown as black dots. The 21.5° contour is shown to highlight temperature variability at the bloom site.

buoys in this region (Figure 10) and with the observations of *Shcherbina et al.* [2009, 2010] of multiple layered intrusions occurring at the front.

[40] At its peak, several days prior to the cruise sampling, the chlorophyll bloom extended over the region covered by the two main transects (Figure 1). During the time of the cruise, the most biologically active area occurred slightly east of the "salinity plug" stations in transect 1 (Figure 8) where elevated abundance of DDAs was observed. The phytoplankton assemblage was composed of *Hemiaulus* (~60%), *Mastogloia* (~35%), and *Rhizosolenia/Richelia* (~5%) [*Villareal et al.*, 2012]. The nitrogen fixation rates measured were quite low $(0.02–2.37 \text{ nmol N} \, l^{-1} \, d^{-1})$ [*Watkins-Brandt et al.*, 2011], but biogenic silica stock and production rates were high, and the rate of biogenic silica export at depth (300 m) was among the highest ever observed in the NPSG [*Krause et al.*, 2012, 2013].

3.5. KM09 Cruise

3.5.1. 145°W Bloom

[41] The KM09 cruise made a transect through the region of a chlorophyll bloom approximately 3 weeks after its collapse, hence in postbloom conditions (Figure 12). The SSHA associated with the initial bloom ranged from −2 to −6 cm, and the bloom was not focused within eddy centers.

[42] The bloom occurred in the eastern part of the general study area, i.e., in the area where the STF curves southward, and the front can be observed in a longitudinal transect. This bloom site, centered at 26°N, was significantly south of the characteristic bloom location of ~30°N latitude. Consequentially, the salinities here were higher, with most surface salinities > 35 (Figure 13). There was a large amount of variability in the subsurface (to 200 m) salinity structure, as well as spikes in the surface salinity gradient, suggesting that it was at the frontal zone. Throughout the section, there was a SSM between 75 and 200 m depth. Phosphate was at the level of
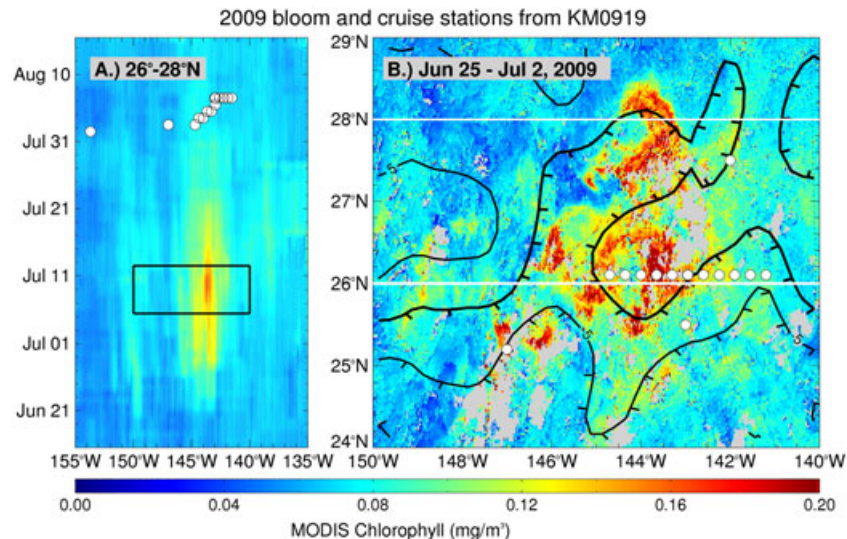
Figure 12. Hovmöller diagram of (a) MODIS chlorophyll showing the development of the 2009 145°W bloom and (b) an 8 day composite (5–12 July) showing the maximum extent of the chlorophyll bloom, overlain with station locations (circles) and SSHA contours. The zero contour is thicker. The zero and negative contours have hash marks indicating the direction of negative values. The contour interval is 5 cm. The black lines in Figure 12a depict the temporal and longitudinal extent of the data shown in Figure 12b, and the white lines in Figure 12b depict the latitude range of the data shown in Figure 12a. Gray areas have missing data due to cloud coverage.
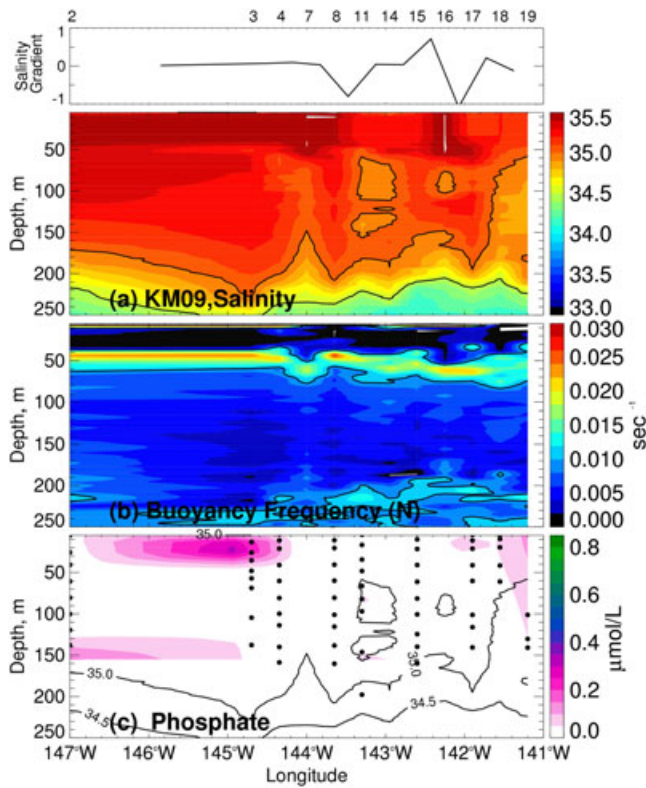
Figure 13. Sections of (a) salinity (PSU), (b) the buoyancy frequency, N (s^{-1}), and (c) phosphate (μM), from KM09. The station sampling in shown by the station numbers along the top of Figure 13a and by positions of the bottle samples marked by the black dots in Figure 13c. Black lines show the 34.5 and 35.0 isohalines. The surface salinity gradient (PSU/degree longitude) is shown above Figure 13a.

detection (~0.05 μM) throughout the section, indicating that the phosphacline was below the deepest sample depths (~150 m). Diatom abundance and biogenic silica concentrations were very low across the transect, indicating that the bloom was completely terminated [*Krause et al.*, 2013; *Villareal et al.*, 2012].

3.5.2. 155°W Bloom

[43] The 155°W bloom is the only bloom of the five discussed in this paper that was sampled at its peak, according to the satellite chlorophyll data (Figure 14). The SSHA associated with the initial bloom ranged from −6 to 0 cm. The bloom sampled was not focused within an eddy, although another bloom south of it (21–23°N) was focused with an SSH depression.

[44] The bloom was developing as the ship was returning to Hawaii, and the route back was diverted to sample it. The diatom abundance at these two stations was several orders of magnitude larger than background levels, and the bloom was dominated by the diatom *Mastogloia woodiana* and other small pennate diatoms with significant numbers of *Hemiaulus hauckii* [*Villareal et al.*, 2012]. Given that only two stations were occupied in this area, it is not possible to assess whether a front occurred at this location from the station data. However, there was no indication of a front in the underway salinity data, and the location was several degrees both south and east of the climatological location of the STF (Figure 1). There was a SSM in the area which can be seen in the data from an Argo float that drifted along 26°N just north of the bloom stations (Figure 15b). There was also a significant intrusion of lower-salinity water at 50–150 m depth, coincident with the initiation of the chlorophyll bloom (Figure 15a). This feature is much less pronounced in the temperature data (Figure 15c).
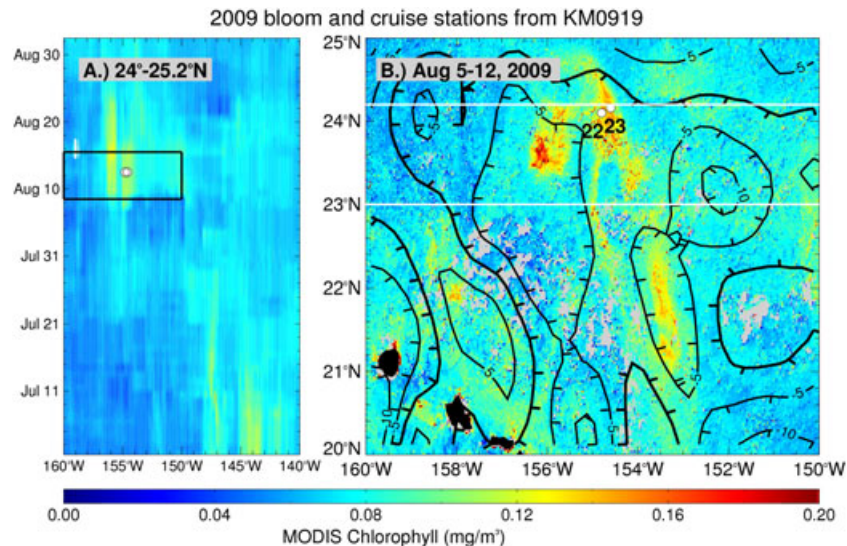
Figure 14. Hovmöller diagram of (a) MODIS chlorophyll showing the development of the 2009 155°W bloom and (b) an 8 day composite (5–12 Aug) showing the maximum extent of the chlorophyll bloom, overlain with station locations (circles) and SSHA contours. The zero contour is thicker. The zero and negative contours have hash marks indicating the direction of negative values. The contour interval is 5 cm. The black lines in Figure 14a depict the temporal and longitudinal extent of the data shown in Figure 14b, and the white lines in Figure 14b depict the latitude range of the data shown in Figure 14a. Gray areas have missing data due to cloud coverage.
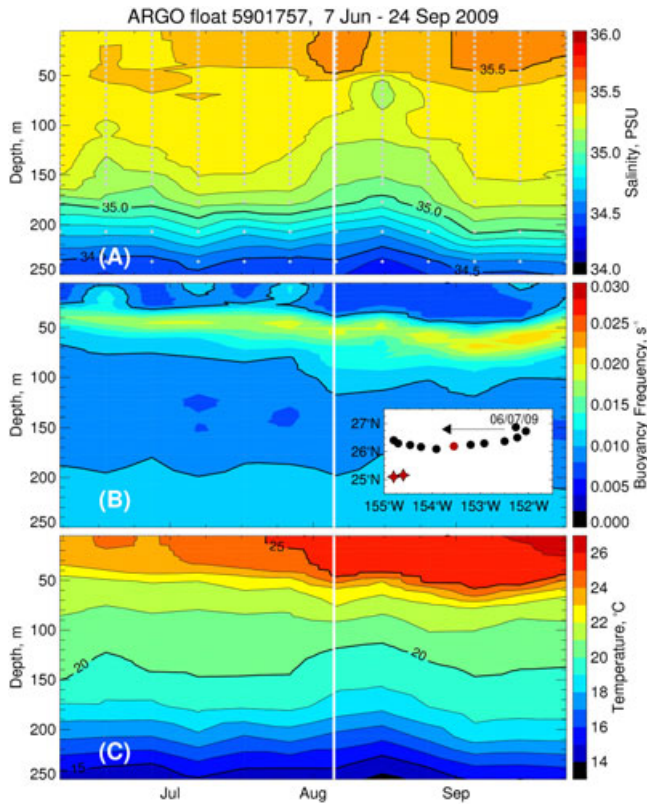
Figure 15. Sections of (a) salinity (PSU), (b) the buoyancy frequency N (s^{-1}), and (c) temperature ($^{\circ}$C) from Argo float 5901757 for June–September 2009. The white line indicates the timing of the initiation of the chlorophyll bloom at 155°W. The map inset in Figure 15b shows float profiles (circles) and the locations of the 2009 bloom stations (red diamonds). The float drifted due west along 26°N. The red dot indicates the location of the float profile synoptic with the station sampling.

4. Discussion

4.1. Eddies

[45] Elevated chlorophyll in the four of the five blooms examined here was predominately associated with low absolute SSHA, consistent with previous descriptions [*Calil et al.*, 2011; *Calil and Richards*, 2010; *Guidi et al.*, 2012; *Wilson and Qiu*, 2008]. The 2008 bloom occurred within an anticyclonic eddy (Table 2), which typically does not have elevated biomass associated with it, or if it does, it occurs in the upwelling zone on the outside edge of the eddy, not in the center [*Yentsch and Phinney*, 1985]. However, a number of studies have reported elevated levels of nitrogen fixation and/or elevated abundances of diazotrophs in the center of anticyclonic eddies [*Davis and McGillicuddy*, 2006; *Fong et al.*, 2008; *Holl et al.*, 2007], although the mechanisms for this association are unknown. *Fong et al.* [2008] speculated on a number of reasons, including that shear along the periphery of the eddy enhanced diapycnal nutrient exchange. The shoaling of the phosphacline (Figure 9c) did occur at the eddy periphery, consistent with this mechanism. However, it is curious that at the ALOHA station increases in nitrogen fixation are observed with elevated SSHA of anticylconic eddies, but not with cyclonic eddies that should provide a more consistent nutrient upwelling [*Church et al.*, 2009]. Clearly, the impacts of mesoscale features on the nutrient field and on the phytoplankton in the NPSG are not straightforward and require a better understanding.

4.2. STF

[46] Four of the five blooms occurred near a salinity front associated with the STF (Table 2), although the front was not always evident at the surface. The surface salinity front and the subsurface salinity front do not always coincide and can be offset by several degrees of latitude (Figures 2 and 7). The small bloom in 2009 at 155°W developed too far south (25°N) to be associated with the STF. While the Hawaii blooms are too far south to be associated with the STF, some of the blooms in the southern region appear to be driven by frontal dynamics between eddies [*Guidi et al.*, 2012].

[47] Changes in the phosphacline associated with the STF could be playing a role in the development of the 30°N blooms. While a sharp shoaling of the phosphacline occurs between 35°N and 40°N [*Hayward et al.*, 1983; *Pak et al.*, 1988], at the STF at 30°N, the shoaling is much more gradual and sometimes does not occur (Figure 2). There is a difference in distribution between nitrate and phosphate across the STF (Figure S1). A small increase in surface phosphate levels occurs on the northern side of the STF, but not in nitrate levels (Figure S1). An indication of this dynamic was also seen in transect 1 from the 2008 cruise, which had an intrusion of fresher water with elevated phosphate levels, but not nitrate levels (Figures 9c and S3). Dynamics that inject phosphate into the surface waters in the bloom region could stimulate blooms of diazotrophs and DDAs. Water between 100 and 400 m depth in this area is out of Redfield balance, with higher levels of phosphate than the N:P Redfield ratio of 16:1 [*Karl and Letelier*, 2008]. *Karl and Letelier* [2008] suggested that the upwelling of this water with excess P is what drives summer blooms of nitrogen-fixing organisms at the station ALOHA. The front can have numerous intrusions of relatively cold and fresh water in the upper 100 m [*Shcherbina et al.*, 2010]. These lateral injections of water across the front could be transporting phosphate if they are occurring in conjunction with a shoaling phosphacline across the STF (Figure 2).

Table 2. Summary of Characteristics of the Five Blooms

Year	Bloom Location	Bloom Stage	At Front?	SSM?[a]	Eddy Center?
2002	148–154°W, 30–33°N	initiation	Y	Y	N
2007	158°W, 31°N	prebloom	Y	N	N
2008	138–141°W, 30–32°N	decline	Y	Y	Y
2009	143–146°W, 25–28°N	postbloom	Y	Y	N
	155°W, 25°N	peak	N	Y	N

[a]SSM = subsurface stratification minimum.

4.3. Nutrients

[48] Varying amounts of excess phosphate were observed during the different cruises (Figure 16a). Excess phosphate, P_{ex}, defined as $P_{ex} = P - NO_3/16$ (and only calculated when NO_3 was greater than zero) ranged from 0 to 0.3 $\mu mol\,kg^{-1}$ for the three cruises. The highest values of P_{ex} were measured during the 2002 cruise, and these occurred throughout the upper 200 m. Lower P_{ex} values were seen in 2008, and in 2009 the values were mostly < 0.05. This pattern of variability is consistent with the timing of the samples relative to the bloom's development. For example, the stations in 2002, the year with the highest P_{ex} values, were sampled synoptically with the chlorophyll bloom as observed with satellite data, but higher chlorophyll values developed at the station locations several weeks after the cruise (Figure 3). In other words, the P_{ex} measured during the RoMP02 cruise could have been used to fuel a developing bloom of diazotrophs. In contrast, in both 2008 and 2009, the area was sampled postbloom, and P_{ex} values were lower. From data collected during the 2008 cruise, *Duhamel et al.* [2010] concluded that the autotrophic picoplankton biomass (0.2–2.0 μm) was primarily limited by nitrogen, but *Watkins-Brandt et al.* [2011] concluded that nitrogen fixation ($>10\,\mu m$ net plankton diazotrophic symbioses abundant) was limited by phosphate. The supply of Si does not appear to be a driving force behind the blooms in this region. In the surface waters (0–150 m), there is an excess of Si relative to N and P (Figure 16b), and data from the 2008 and 2009 cruises indicate that diatom growth was not limited by silicon availability [*Krause et al.*, 2012, 2013].

### 4.4. Critical Latitude and Stratification Minimum

[49] It has been suggested that dynamics associated with the critical latitude at 30°N cause IWs generated at the Hawaiian Ridge to break in the subsurface, providing a pulse of nutrients to fuel the chlorophyll blooms [*Wilson*, 2011]. *Shrira and Townsend* [2010] described a mechanism where IWs could penetrate several hundreds of kilometers northward of the critical latitude in waveguides where the stratification was at a local minimum. *Wilson* [2011] invoked this singular

Figure 16. Profiles of (a) excess PO_4 (PO_4-$NO_3/16$) and (b) excess SiO_4 (SiO_4-NO_3) for all stations from the 2002 (black), 2008 (blue), and 2009 (green) cruises.

focusing mechanism to explain the frequent development of blooms slightly north of the critical latitude. However, the stratification value ($3 \times 10^{-4}\,s^{-1}$) used by *Shrira and Townsend* [2010] is an order of magnitude weaker than the values in the North Pacific ($5 \times 10^{-3}\,s^{-1}$). Using the observed stratification value in their calculation [*Shrira and Townsend*, 2010, equation 3.9] does not result in any significant northward penetration of IWs past the 30°N critical latitude. While this suggests that *Shrira and Townsend*'s [2010] singular focusing mechanism is not as relevant as *Wilson* [2011] argued, the observed SSMs are still important as they will facilitate turbulent mixing, regardless of the cause.

[50] All of the bloom sites had a SSM, except the 2007 bloom (Table 2). The absence of an observed SSM could be an issue of timing and/or location. It is possible that a SSM was missed due to the localized sampling of the cruise. Data from the WOCE cruises show that the SSM occurred on the north side of the front (Figure 2). The 2007 bloom actually developed slightly west of the 2007 cruise study area (Figure 6), and it is also possible that spatial heterogeneity plays a role. For example, the salinity intrusions mapped in detail during the STF07 cruise had cross-frontal spatial scales of variability of the order of 10–30 km [*Shcherbina et al.*, 2010].

[51] The generation of enhanced mixing at a SSM will not necessarily lead to nutrient injection into the surface water and subsequent bloom initiation. There are other conditions that must be met. The nutricline, specifically the phosphacline (assuming that the blooms are composed of diazotrophs or DDAs), needs to coincide with the SSM, and the SSM needs to be shallow enough that it is in contact with the base of the mixed layer. Vertical profiles indicating different relationships between these parameters are shown in Figure 17. The stratification profiles are taken from Argo float data and were selected using the variation in their vertical distributions. The nutrient data are from two stations from the 2002 cruise and were selected because they best depict the range of nutricline depths in the region, from a minimum of ~100 m to a maximum of ~200 m. The "perfect storm" of conditions is depicted in Figure 17a, where the shallowest nutricline intersects with the SSM, which is just below the mixed layer (ML). The nutricline can intersect with the SSM, but if the SSM is isolated from the ML, upward mixing of phosphate will not reach phytoplankton in the ML (Figure 17b). If the SSM exists above the nutricline, enhanced mixing there will not entrain nutrients into the ML (Figure 17c). Sometimes there is no SSM (Figure 17d).

[52] Another consideration is that the injection of phosphate must be into a layer where there is enough light for nitrogen fixation, a process which is considered to have higher light requirements than nondiazotrophic photosynthesis [*Capone et al.*, 1997; *LaRoche and Breitbarth*, 2005]. The depth of the euphotic zone (depth of 1% surface irradiance) measured on the 2008 and 2009 cruises ranged between 84 and 142 m, well below the MLD. Most of the studies looking at light requirement for diazotrophs [*Bell and Fu*, 2005; *Breitbarth et al.*, 2008] focused on *Trichodesmium*, which does not play a dominant role at 30°N in the Pacific [*Venrick*, 1997; *Villareal et al.*, 2011]. A study of the light requirements of the DDA *Hemiaulus hauckii* [*Pyle*, 2011] indicates that its compensation depth falls within the observed euphotic zone in 2008 and 2009 and that growth rate saturation
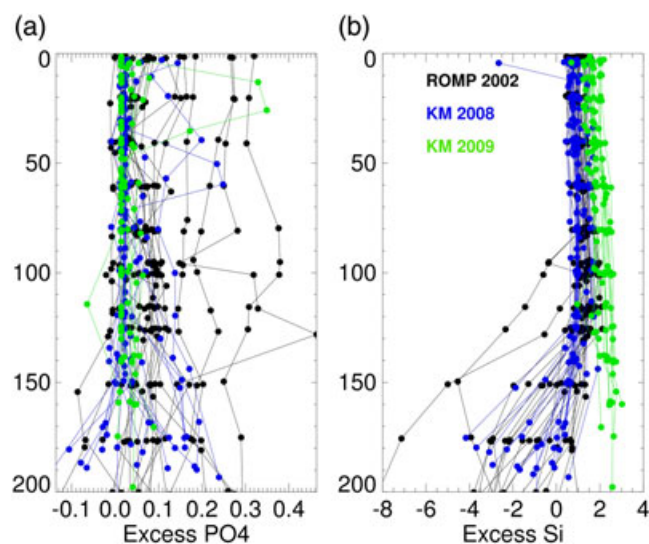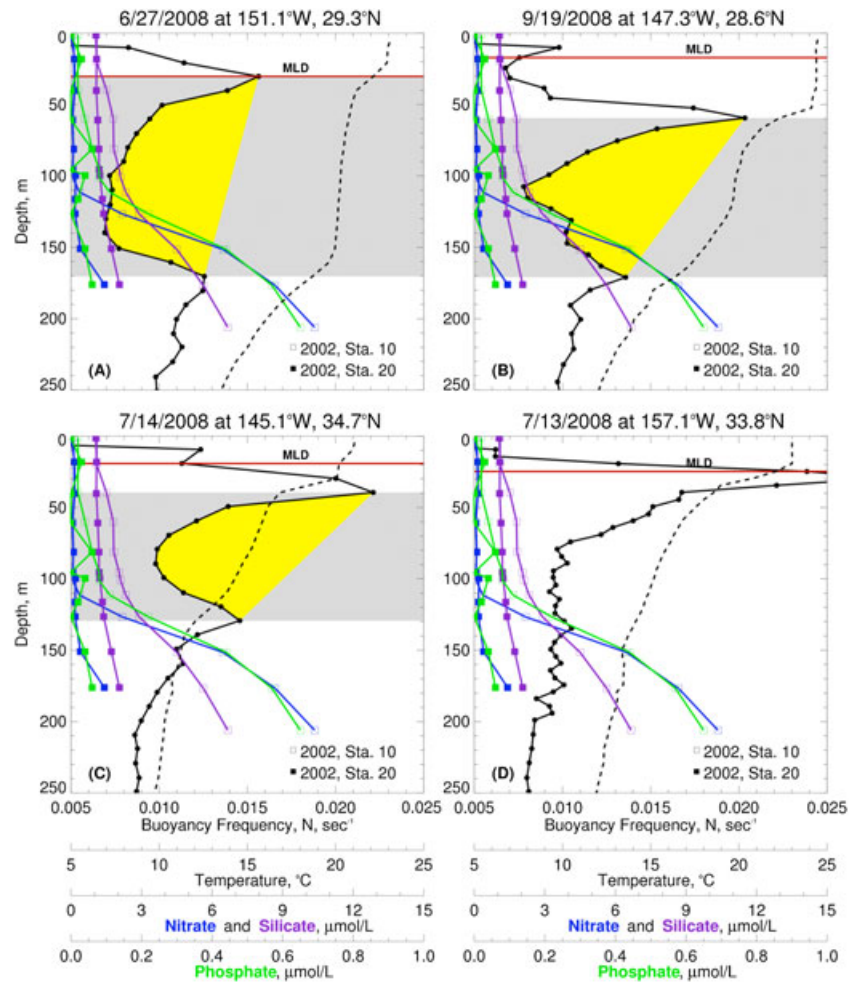
Figure 17. Profiles of stratification (buoyancy frequency, $N\,(\mathrm{s}^{-1})$, shown in solid black) and temperature (dashed black) from Argo floats, overlain with nitrate (blue), phosphate (green), and silicate (purple) profiles from two stations during RoMP02, one with a relatively shallow nutricline near 100 m depth and one with a deeper nutricline below 180 m depth. The selected profiles depict different interactions between the nutricline, the subsurface stratification minimum (SSM, shaded yellow), and the ML (red). (a) The SSM coincides with the nutricline and is just below the ML, conditions that could result in nutrients getting into the ML. (b) The SSM is cut off from the ML, and vertical mixing within the SSM will not deliver nutrients into the ML. (c) The SSM lies above the nutricline, and enhanced mixing within it will not modify the nutrient distribution. (d) There is no SSM to stimulate vertical mixing. The vertical extent of the SSM is shaded gray on the plots to illustrate its position relative to the nutrient profiles.

occurred at ~100 µmol photons $\mathrm{m}^{-2}\,\mathrm{s}^{-1}$ or approximately 5% incident (50–80 m depth), so light limitation is probably not a factor controlling the development of the summer blooms in the NPSG.

[53] Another factor is the specific mechanism driving the mixing at the SSM. If the mechanism is the breaking of IWs, variation in their energy and amplitude will impact the strength of the mixing generated by their breaking. Considerable temporal variation has been observed in the generation and amplitude of IWs along the Hawaiian Ridge [*Powell et al.*, 2012; *Zilberman et al.*, 2011]. In addition to breaking IWs, there are other mechanisms that could generate enhanced mixing, such as frontal trapping of IWs [*Kunze and Sanford*, 1984], mesoscale straining of IWs [*Bühler and McIntyre*, 2005], and parametric subharmonic instability [*MacKinnon and Winters*, 2005]. Clearly, the conditions can exist in the bloom region where subsurface

mixing will bring nutrients into the ML. However, the conditions (a significant mixing event and a vertical intersection of the phosphacline and SSM) are not always right for this to occur, which is consistent with the sporadic blooms observed in the satellite chlorophyll data. Mixing events are likely a highly episodic occurrence, making them difficult to observe during ship surveys. The physiology of the larger phytoplankton in this area indicates that they experience time-variable changes in growth [*Li et al.*, 2011], which would be consistent with episodic pulses of nutrients from breaking IWs.

[54] The mixing scenario described here (Figure 17a) could happen at either of the two areas, Hawaii 30°N and Hawaii. However, the STF, which can be associated with a shoaling phosphacline, will only have an impact on the 30°N region. Breaking IWs can happen anywhere, and while substantial conversion of IW energy has been observed near

Hawaii [*Carter and Gregg*, 2006; *Xie et al.*, 2011], the 30°N region is a mixing "hotspot" from IW activity [*MacKinnon et al.*, 2013; *Wilson*, 2011]. Both of these factors probably contribute to there being stronger and more frequent blooms at 30°N relative to Hawaii [*Dore et al.*, 2008; *Krause et al.*, 2013; *Wilson and Qiu*, 2008].

5. Conclusions

[55] We have used cruise data and Argo float data to characterize the hydrography associated with blooms in the 30°N region of the North Pacific. The subsurface salinity data of all of the four blooms indicated that they occurred at the STF zone. There is often heterogeneity in the vertical structure of the STF. The surface (0 to ~50 m depth) expression of the salinity front can be displaced by several hundreds of kilometers from the subsurface (100–200 m depth) salinity front. Nutrient changes across the STF are not dramatic. Sometimes the nutricline shoals slightly across the STF, and sometimes it does not. A surface increase in phosphate, but not nitrate, appears sometimes in the surface water north of the STF. On both sides of the STF, water between 100 and 400 m depth deviates from the canonical 16:1 N:P Redfield ratio, with higher levels of phosphate and lower N:P. Injection of these phosphate-enriched waters into the ML in the bloom region could stimulate blooms of diazotrophic organisms.

[56] It is hypothesized that breaking IWs in the region of the critical latitude (30°N) generate nutrient fluxes that fuel the summer blooms of chlorophyll that are frequently observed in this region by satellites. The observational data indicate that the conditions required for this to happen are a subsurface minimum in stratification coinciding vertically with the nutricline, and which is not isolated from the ML. With these conditions, the breaking of a strong IW would result in mixing of nutrients into the ML. The combination of factors will not always occur simultaneously, consistent with the sporadic nature of the development of the blooms.

[57] Sampling the blooms is problematic given their somewhat variable timing (a 2–3 month window), their considerable distance from shore, and the difficulty of securing funding for what is perceived as a risky venture. Equipping gliders and Argo floats with chemical and biological sensors would provide additional in situ data needed to clarify the specific mechanisms that drive these blooms. This question should also be addressed by ocean modeling, but it will require a model that can accurately resolve eddies, nutrients fields, internal waves, as well as the biology.

References

Behrenfeld, M. J. (2010), Abandoning Sverdrup's critical depth hypothesis on phytoplankton blooms, *Ecology 91*, 977–989.

Bell, P. R. F., and F.-X. Fu (2005), Effect of light on growth, pigmentation and N_2 fixation of cultured *Trichodesmium* sp. from the Great Barrier Reef lagoon, *Hydrobiologia*, *543*, 25–35.

Benitez-Nelson, C. R., and D. J. McGillicuddy, Jr. (2008), Mesoscale physical-biological-biogeochemical linkages in the open ocean: An introduction to the results of the E-Flux and EDDIES programs *Deep-Sea Res., II*, *55*, 1133–1138.

Breitbarth, E., J. Wohlers, J. Klaes, J. LaRoche, and I. Peeken (2008), Nitrogen fixation and growth rates of *Trichodesmium* IMS-101 as a function of light intensity, *Mar. Ecol. Prog. Ser.*, *359*, 25–36.

Brzezinski, M. A., J. W. Krause, M. J. Church, D. M. Karl, B. Li, J. L. Jones, and B. Updyke (2011), The annual silica cycle of the North Pacific subtropical gyre, *Deep-Sea Res., I*, *58*, 988–1001.

Bühler, O., and M. E. McIntyre (2005), Wave capture and wave-vortex duality, *J. Fluid Mech.*, *534*, 67–95.

Calil, P. H. R., S. C. Doney, K. Yumimoto, K. Eguchi, and T. Takemura (2011), Episodic upwelling and dust deposition as bloom triggers in low-nutrient, low-chlorophyll regions, *J. Geophys. Res.*, *116*, doi:10.1029/2010JC006704.

Calil, P. H. R., and K. J. Richards (2010), Transient upwelling hot spots in the oligotrophic North Pacific, *J. Geophys. Res.*, *115*, doi:10.1029/2009JC005360.

Capone, D. G., J. P. Zehr, H. W. Paerl, B. Bergman, and E. J. Carpenter (1997), *Trichodesmium*, a globally significant marine cyanobacterium, *Science*, *276*, 1221–1229.

Carter, G. S., and M. C. Gregg (2006), Persistent near-diurnal internal waves observed above a site of M2 barotropic-to-baroclinic conversion, *J. Phys. Oceanogr.*, *36*, 1136–1147.

Chiswell, S. M. (2011), Annual cycles and spring blooms in phytoplankton: Don't abandon Sverdrup completely, *Mar. Ecol. Prog. Ser.*, *443*, 39–50.

Church, M. J., C. Mahaffey, R. M. Letelier, R. Lukas, J. P. Zehr, and D. M. Karl (2009), Physical forcing of nitrogen fixation and diazotroph community structure in the North Pacific subtropical gyre, *Global Biogeochem. Cy.*, *23*, doi:10.1029/2008GB003418.

Davis, C. S., and D. J. McGillicuddy, Jr. (2006), Transatlantic abundance of the N_2-fixing colonial cyanobacterium *Trichodesmium, Science*, *312*, 1517–1520.

Dore, J. E., R. M. Letelier, M. J. Church, and D. M. Karl (2008), Summer phytoplankton blooms in the oligotrophic North Pacific subtropical gyre: Historical perspective and recent observations, *Prog. Oceanogr.*, *76*, 2–38.

Duhamel, S., S. T. Dyhrman, and D. M. Karl (2010), Alkaline phosphatase activity and regulation in the North Pacific Subtropical Gyre, *Limnol. Oceanogr.*, *55*, 1414–1425.

Fong, A. A., D. M. Karl, R. Lukas, R. M. Letelier, J. P. Zehr, and M. J. Church (2008), Nitrogen fixation in an anticyclonic eddy in the oligotrophic North Pacific Ocean, *ISME J.*, *2*, 663–676.

Franks, P. J. S. (1992), Phytoplankton blooms at fronts: Patterns, scales and physical forcing mechanisms, *Reviews in Aquatic Sciences*, *6*, 121–137.

Guidi, L., et al., (2012), Does eddy-eddy interaction control surface phytoplankton distribution and carbon export in the North Pacific Subtropical Gyre?, *J. Geophys. Res.*, *117*, doi:10.1029/2012JG001984.

Hayward, T. L., E. L. Venrick, and J. A. McGowan (1983), Environmental heterogeneity and plankton community structure in the central North Pacific, *J. Mar. Res.*, *41*, 711–729.

Heinbokel, J. F. (1986), Occurrence of *Richelia intracellularis* (Cyanophyta) within the diatoms *Hemiaulus haukii* and *H. membranaceus* off Hawaii, *J. Phycol.*, *22*, 399–403.

Holl, C. M., A. M. Waite, S. Pesant, P. A. Thompson, and J. P. Montoya (2007), Unicellular diazotrophy as a source of nitrogen to Leeuwin Current coastal eddies, *Deep-Sea Res., II*, *54*, 1045–1054.

Karl, D., A. Michaels, B. Bergman, D. Capone, E. Carpenter, R. M. Letelier, F. Lipschultz, H. Paerl, D. Sigman, and L. Stal (2002), Dinitrogen fixation in the world's ocean, *Biogeochem.*, *56/57*, 47–98.

Karl, D. M., M. J. Church, J. E. Dore, R. M. Letelier, and C. Mahaffey (2012), Predictable and efficient carbon sequestration in the North Pacific Ocean supported by symbiotic nitrogen fixation, *P. Natl. Acad. Sci. USA*, *109*, 1842–1849.

Karl, D. M., and R. M. Letelier (2008), Nitrogen fixation-enhanced carbon sequestration in low nitrate, low chlorophyll seascapes, *Mar. Ecol. Prog. Ser.*, *364*, 257–268.

Karl, D. M., R. M. Letelier, D. V. Hebel, D. F. Bird, and C. D. Winn (1992), *Trichodesmium* Blooms and New Nitrogen in the North Pacific Gyre, in Marine Pelagic Cyanobacteria: *Trichodesmium* and Other Diazotrophs, edited by E. J. Carpenter, *et al.*, pp. 219–237, Kluwer Academic, Dordrecht.

Krause, J. W., M. A. Brzezinski, T. A. Villareal, and C. Wilson (2012), Increased kinetic efficiency for silicic acid uptake as a driver of summer diatom blooms in the North Pacific subtropical gyre, *Limnol. Oceanogr.*, *57*, 1084–1098.

Krause, J. W., M. A. Brzezinski, T. A. Villareal, and C. Wilson (2013), Biogenic silica cycling during summer phytoplankton blooms in the North Pacific subtropical gyre, *Deep-Sea Res., I*, *71*, 49–60.

Kunze, E., and T. B. Sanford (1984), Observations of near-inertial waves in a front, *J. Phys. Oceanogr.*, *14*, 566–581.

Landry, M. R. (2002), Integrating classical and microbial food web concepts: Evolving views from the open-ocean tropical Pacific, *Hydrobiologia*, *480*, 29–39.

LaRoche, J., and E. Breitbarth (2005), Importance of the diazotrophs as a source of new nitrogen in the ocean, *J. Sea Res.*, *53*, 67–91.

Laurs, R. M., and R. J. Lynn (1977), Seasonal migration of North Pacific albacore, *Thunnus alalunga*, into North American coastal waters: Distribution, relative abundance, and association with transition zone waters, *Fish. Bull.*, *75*, 795–822.

Letelier, R. M., D. M. Karl, R. Lukas, and T. Strub (2000), Role of late winter mesoscale events in the biogeochemical variability of the upper water column of the North Pacific Subtropical Gyre, *J. Geophys. Res.*, *105*, 28,723–28,739.

Li, B., D. M. Karl, R. M. Letelier, and M. J. Church (2011), Size-dependent photosynthetic variability in the North Pacific Subtropical Gyre, *Mar. Ecol. Prog. Ser.*, *440*, 27–40.

Liu, C.-C., and J. Woods (2004), Deriving four parameters from patchy observations of ocean color for testing a plankton ecosystem model *Deep-Sea Res., II*, *51*, 1053–1062.

Lynn, R. J. (1986), The subarctic and northern subtropical fronts in the eastern North Pacific Ocean in spring, *J. Phys. Oceanogr.*, *16*, 209–222.

MacKinnon, J. A., M. H. Alford, R. Pinkel, J. Klymak, and Z. Zhao (2013), The latitudinal dependence of shear and mixing in the Pacific transiting the critical latitude for PSI, *J. Phys. Oceanogr.*, *43*, 3–16.

MacKinnon, J. A., and K. B. Winters (2005), Subtropical catastrophe: Significant loss of low-mode tidal energy at 28.9°, *Geophys. Res. Lett.*, *32*, doi:10.1029/2005GL023376.

Niiler, P. P., and R. W. Reynolds (1984), The three-dimensional circulation near the eastern North Pacific Subtropical Front, *J. Phys. Oceanogr.*, *14*, 217–230.

Olson, D. B. (2002), Biophysical dynamics of ocean fronts, in Biological-Physical Interactions in the Sea, edited by A. R. Robinson, *et al.*, pp. 187–218, John Wiley & Sons, Inc., New York.

Pak, H., D. A. Kiefer, and J. C. Kitchen (1988), Meridional variations in the concentration of chlorophyll and microparticles in the North Pacific Ocean, *Deep-Sea Res.*, *35*, 1151–1171.

Pilskaln, C. H., T. A. Villareal, M. Dennett, C. Darkangelo-Wood, and G. Meadows (2005), High concentrations of marine snow and diatom algal mats in the North Pacific Subtropical Gyre: Implications for carbon and nitrogen cycles in the oligotrophic ocean, *Deep-Sea Res., I*, *52*, 2315–2332.

Powell, B. S., I. Janeković, G. S. Carter, and M. A. Merrifield (2012), Sensitivity of internal tide generation in Hawaii, *Geophys. Res. Lett.*, *39*, 10.1029/2012GL051724.

Pyle, A. (2011), Light dependent growth and nitrogen fixation rates in the *Hemiaulus hauckii* and *Hemiaulus membranaceus* diatom-diazotroph associations, M.S. thesis, 79 pp.

Roden, G. I. (1971), Aspects of the transition zone in the northeastern Pacific *J. Geophys. Res.*, *76*, 3462–3475.

Roden, G. I. (1974), Thermohaline structure, fronts, and sea-air energy exchange of the trade wind region east of Hawaii, *J. Phys. Oceanogr.*, *4*, 168–182.

Roden, G. I. (1975), On North Pacific temperature, salinity, sound velocity and density fronts and their relation to the wind and energy flux fields, *J. Phys. Oceanogr.*, *5*, 557–571.

Roden, G. I. (1980), On the subtropical frontal zone north of Hawaii during winter, *J. Phys. Oceanogr.*, *10*, 342–362.

Samelson, R. M., and C. A. Paulson (1988), Towed thermistor chain observations of fronts in the subtropical North Pacific, *J. Geophys. Res.*, *93*, 2237–2246.

Saur, J. F. T. (1980), Surface salinity and temperature on the San Francisco-Honolulu route June 1966-December 1970 and January 1972-December 1975, *J. Phys. Oceanogr.*, *10*, 1669–1680.

Seki, M. P., J. J. Polovina, D. R. Kobayashi, R. R. Bidigare, and G. T. Mitchum (2002), An oceanographic characterization of swordfish (*Xiphias gladius*) longline fishing grounds in the subtropical North Pacific, *Fish. Oceanogr.*, *11*, 251–266.

Shcherbina, A. Y., M. C. Gregg, M. H. Alford, and R. R. Harcourt (2009), Characterizing thermohaline intrusions in the North Pacific subtropical frontal zone, *J. Phys. Oceanogr.*, *39*, 2735–2756.

Shcherbina, A. Y., M. C. Gregg, M. H. Alford, and R. R. Harcourt (2010), Three-dimensional structure and temporal evolution of submesoscale thermohaline intrusions in the North Pacific subtropical frontal zone, *J. Phys. Oceanogr.*, *40*, 1669–1689.

Shrira, V. A., and W. A. Townsend (2010), Inertia-gravity waves beyond the inertial latitude. Part 1. Inviscid singular forcing, *J. Fluid Mech.*, *664*, 478–509.

Singler, H. R., and T. A. Villareal (2005), Nitrogen inputs into the euphotic zone by vertically migrating *Rhizosolenia* mats, *J. Plankton Res.*, *27*, 545–556.

Sohm, J. A., A. Subramaniam, T. E. Gunderson, E. J. Carpenter, and D. G. Capone (2011), Nitrogen fixation by *Trichodesmium* spp. and unicellular diazotrophs in the North Pacific Subtropical Gyre, *J. Geophys. Res.*, *116*, doi:10.1029/2010JG001513.

Stumpf, R. P., R. W. Litaker, L. Lanerolle, and P. A. Tester (2008), Hydrodynamic accumulation of *Karenia* off the west coast of Florida, *Cont. Shelf Res.*, *28*, 189–213.

Talley, L. D., T. M. Joyce, and R. A. deSzoeke (1991), Trans-Pacific sections at 47°N and 152°W: distribution of properties in the subpolar gyre, *Deep-Sea Res.*, *38*, S68–S82.

Tsuchiya, M., and L. D. Talley (1996), Water-property distributions along an eastern Pacific hydrographic section at 135W, *J. Mar. Res.*, *54*, 541–564.

Venrick, E. L. (1974), The distribution and significance of *Richelia intracellularis* Schmidt in the North Pacific central gyre, *Limnol. Oceanogr.*, *19*, 437–445.

Venrick, E. L. (1993), Phytoplankton seasonality in the central North Pacific: The endless summer reconsidered, *Limnol. Oceanogr.*, *38*, 1135–1149.

Venrick, E. L. (1997), Comparison of the phytoplankton species composition and structure in the Climax area (1973–1985) with that of ALOHA (1994), *Limnol. Oceanogr.*, *42*, 1643–1648.

Villareal, T. A., L. R. Adornato, C. Wilson, and C. A. Schoenbaechler (2011), Summer blooms of diatom-diazotroph assemblages and surface chlorophyll in the N. Pacific gyre - A disconnect, *J. Geophys. Res.*, *116*, doi:10.1029/2010JC006268.

Villareal, T. A., C. G. Brown, M. A. Brzezinski, J. W. Krause, and C. Wilson (2012), Summer diatom blooms in the North Pacific Subtropical Gyre: 2008–2009, *PLoS One*, *7*, doi:10.1371/journal.pone.0033109.

Watkins-Brandt, K. S., R. M. Letelier, Y. H. Spitz, M. J. Church, D. Böttjer, and A. E. White (2011), Addition of inorganic or organic phosphorus enhances nitrogen and carbon fixation in the oligotrophic North Pacific, *Mar. Ecol. Prog. Ser.*, *432*, 17–29.

White, A. E., Y. H. Spitz, and R. M. Letelier (2007), What factors are driving summer phytoplankton blooms in the North Pacific Subtropical Gyre?, *J. Geophys. Res.*, *112*, doi:10.1029/2007JC004129.

Wilson, C. (2003), Late summer chlorophyll blooms in the oligotrophic North Pacific subtropical gyre, *Geophys. Res. Lett.*, *30*, doi:10.1029/2003GL017770.

Wilson, C. (2011), Chlorophyll anomalies along the critical latitude at 30°N in the NE Pacific, *Geophys. Res. Lett.*, *38*, doi:10.1029/2011GL048210.

Wilson, C., and X. Qiu (2008), Global distribution of summer chlorophyll blooms in the oligotrophic gyres, *Prog. Oceanogr.*, *78*, 107–134.

Wilson, C., T. A. Villareal, N. Maximenko, S. J. Bograd, J. P. Montoya, and C. A. Schoenbaechler (2008), Biological and physical forcings of late summer chlorophyll blooms at 30°N in the oligotrophic Pacific, *J. Mar. Sys.*, *69*, 164–176.

Xie, X. H., X. D. Shang, H. von Haren, G. Y. Chen, and Y. Z. Zhang (2011), Observations of PSI-induced near-inertial waves equatorward of the critical diurnal latitude, *Geophys. Res. Lett.*, *38*, doi:10.1029/2010GL046521.

Yentsch, C. S., and D. A. Phinney (1985), Rotary motions and convection as a means of regulating primary production in warm core rings, *J. Geophys. Res.*, *90*, 3237–3248.

Yoder, J. A., S. G. Ackleson, R. T. Barber, P. Flament, and W. M. Balch (1994), A line in the sea, *Nature*, *371*, 689–692.

Zilberman, N. V., M. A. Merrifield, G. S. Carter, D. S. Luther, M. D. Levine, and T. J. Boyd (2011), Incoherent nature of M_2 internal tides at the Hawaiian Ridge, *J. Phys. Oceanogr.*, *41*, 2021–2036.